British Journal of Pharmacology (1997) 121, 1429–1437

Properties of the pore-forming $P2X_7$ purinoceptor in mouse NTW8 microglial cells

[1]I.P. Chessell, A.D. Michel & P.P.A. Humphrey

Glaxo Institute of Applied Pharmacology, Department of Pharmacology, University of Cambridge, Tennis Court Road, Cambridge CB2 1QJ

1 We have used whole-cell patch clamping methods to study and characterize the cytolytic $P2X_7$ (P2Z) receptor in the NTW8 mouse microglial cell line.

2 At room temperature, in an extracellular solution containing 2 mM Ca^{2+} and 1 mM Mg^{2+}, 2′- and 3′-O-(4-benzoylbenzoyl)-adenosine-5′-triphosphate (Bz-ATP; 300 μM), or ATP (3 mM), evoked peak whole cell inward currents, at a holding potential of -90 mV, of 549 ± 191 and 644 ± 198 pA, respectively. Current-voltage relationships generated with 3 mM ATP reversed at 4.6 mV and did not display strong rectification.

3 In an extracellular solution containing zero Mg^{2+} and 500 μM Ca^{2+} (low divalent solution), brief (0.5 s) application of these agonists elicited larger maximal currents (909 ± 138 and 1818 ± 218 pA, Bz-ATP and ATP, respectively). Longer application of ATP (1 mM for 30 s) produced larger, slowly developing, currents which reached a plateau after approximately 15–20 s and were reversible on washing. Under these conditions, in the presence of ATP, ethidium bromide uptake could be demonstrated. Further applictions of 1 mM ATP produced rapid currents of the same magnitude as those observed during the 30 s application. Subsequent determination of concentration-effect curves to Bz-ATP, ATP and 2-methylthio-ATP yielded EC_{50} values of 58.3, 298 and 505 μM, respectively. These affects of ATP were antagonized by pyridoxal-phosphate-6-azophenyl- 2′, 4′-disulphonic acid (PPADS; 30 μM) but not suramin (100 μM).

4 In low divalent solution, repeated application of 1 mM ATP for 1 s produced successively larger currents which reached a plateau, after 8 applications, of 466% of the first application current. PPADS (30 μM) prevented this augmentation, while 5-(N,N-hexamethylene)-amiloride (HMA) (100 μM) accelerated it such that maximal augmentation was observed after only one application of ATP in the presence of HMA. At a bath temperature of 32°C, current augmentation also occurred in normal divalent cation containing solution.

5 These data demonstrate that mouse microglial NTW8 cells possess a purinoceptor with pharmacological characteristics resembling the $P2X_7$ receptor. We suggest that the current augmentation phenomenon observed reflects formation of the large cytolytic pore characteristic of this receptor. We have demonstrated that pore formation can occur under normal physiological conditions and can be modulated pharmacologically, both positively and negatively.

Keywords: Microglia; $P2X_7$ purinoceptor; pore; ethidium bromide

Introduction

Adenosine 5′-triphosphate (ATP) can cause receptor-mediated permeabilization of membranes in certain cell types, including mast cells (Cockroft & Gomperts, 1979), macrophages (Steinberg *et al*., 1987) and microglia (Ferrari *et al*., 1996). These effects were believed to be mediated by a receptor, originally termed P2Z, which when activated induced membrane permeabilization by formation of large pores, with consequent cytolysis upon persistent receptor activation (Pizzo *et al*., 1992; Chiozzi *et al*., 1996). This receptor was considered distinct from either of the other two major classes of ATP receptors, the P2X and P2Y purinoceptors, on the basis of its unique transductional characteristics (Fredholm *et al*., 1994). However, recently the P2Z receptor has been identified as belonging to the growing family of ionotropic P2X receptors (Surprenant *et al*., 1996), and has consequently been termed $P2X_7$.

Microglial cells are ubiquitously distributed in the brain and functionally they represent the main immune effector cell population of the CNS (see Hofman *et al*., 1989). Microglia are known to release various cytokines, nitric oxide and reactive oxygen species, particularly when activated in a manner analogous to macrophage activation (see McGeer & McGeer, 1995) and, as such, are thought to play a role in various neurodegenerative diseases, including multiple sclerosis (Hofman *et al*., 1989), Parkinson's disease (McGeer *et al*., 1988) and Alzheimer's disease (Rogers *et al*., 1988). Neurones are known to release ATP, either as a transmitter (Wieraszko *et al*., 1989; Edwards *et al*., 1992) or when damaged or lysed. The precise interplay between neuronally-released ATP and microglia is not yet clear. In order to establish whether $P2X_7$ receptors play a key role in the physiological actions of microglia, it is essential to establish the pharmacological and functional properties of these purinoceptors.

In this study we have used whole-cell patch clamping methods to study the characteristics of the $P2X_7$ purinoceptor in a mouse microglial cell line, termed NTW8, derived from a transgenic mouse with an incorporated transgene encoding the immortalizing oncogene, SV40 T-antigen. These cells have the characteristics of primary microglial cells in that they expresss a macrophage specific antigen and release nitric oxide, prostaglandin E_2 and tumour necrosis factor-α (TNF-α) upon activation (Anderson *et al*., 1997).

A preliminary account of some of this work has been presented at a meeting of the British Pharmacological Society (Chessell *et al*., 1997).

Methods

Cell culture

Mouse microglial NTW8 cells were maintained in 75 cm^2 flasks (Costar, Bucks, U.K.), containing Dulbecco's modified

[1] Author for correspondence.

Eagle medium (DMEM) without sodium pyruvate, supplemented with 4.5 mg ml^{-1} glucose, foetal calf serum (10%), N-2 supplement (10 μl ml^{-1}) and basic fibroblast growth factor (bFGF, 10 ng ml^{-1}). They were incubated in a water-saturated atmosphere of 95% O_2/5% CO_2, and passaged when confluent by tripsinization (trypsin-EDTA 1X solution). When required for study, cells were attached to poly-D-lysine (500 μg ml^{-1}) coated glass coverslips (13 mm; Menzel-Glaser, Fisher, Leicester, U.K.) and used for electrophysiological investigations not less than 2 h after plating. Coverslips were used within 2 days.

Electrophysiological recording

For each experiment, coverslips were transferred to a perfused recording chamber (volume approximately 400 μl, flow rate 2 ml min^{-1}) mounted on the stage of an inverted microscope (Nikon Diaphot, Nikon U.K. Ltd., Kingston upon Thames, U.K.). The whole cell configuration of the patch-clamp technique (Hamill *et al*., 1981) was used to record nucleotide-evoked ionic currents. Recordings were made only from ramified microglial cells, thought to reflect the non-activated state (see Kreutzberg, 1996), only where ramifications did not exceed one third of the cell diameter in any direction. Cells were perfused with either normal divalent cation containing solution, consisting of (in mM): NaCl 145, KCl 2, $MgCl_2$ 1, $CaCl_2$ 2, HEPES 10, D-glucose 10 (pH 7.3, osmolarity 300 mOsm), or a low divalent cation solution, identical except for the omission of $MgCl_2$ and the reduction of the $CaCl_2$ concentration to 500 μM. Patch electrodes were pulled from 1.2 mm borosilicate glass (GC120F-10, Clarke Electromedical Supplies, Pangbourne, U.K.), firepolished, and filled with (in mM) Cs aspartate 145, EGTA 11, HEPES 5, NaCl 2 (pH 7.3, osmolarity 290 mOsm). Electrodes had a resistance of 2–5 MΩ when filled with this solution.

Tight seal ($\geqslant$10GΩ) whole-cell currents were recorded with an Axopatch 200B amplifier (Axon Instruments, Foster City, CA, U.S.A.). Currents were filtered with a corner frequency of 1–5 kHz (4-pole Bessel filter), digitized at 2–10 kHz by a Digidata 1200A (Axon Instruments) interface and stored on computer. Only data from cells with a residual series resistance of less than 18 MΩ were analysed and compensation for series resistance was used. Cells were voltage-clamped at $-$90 mV, unless otherwise stated. For voltage-ramp experiments, reported voltages were corrected for the liquid junction potential between the internal solution and the extracellular solution in which zero current was obtained before forming a seal. This correction was made by calculation of the junction potential (Axoscope, Axon Instruments), and subsequent adjustment of the holding potential to take account of this value. All experiments were performed at room temperature (23°C) unless otherwise stated.

Experimental procedures

Several protocols were adopted to investigate the actions of purinoceptor agonists and antagonists. In all cases, agonists were applied by use of a computer-controlled fast-flow U-tube system (Fenwick *et al*., 1982), modified to include an extra solenoid valve, which allowed both rapid application and removal of applied drugs (onset and offset latency approximately 90 and 50 ms, respectively). In all cases where the effects of antagonists or other agents were investigated, these drugs were included at the appropriate concentrations in the U-tube application system.

Initially, in normal divalent cation containing solution, concentration-effect curves to ATP, 2′- and 3′-O-(4-benzoylbenzoyl)-adenosine 5′-triphosphate (Bz-ATP), or 2-methylthio-adenosine 5′-triphosphate (2MeS-ATP) were determined by use of a 2 s agonist application time, with serially increasing agonist concentrations, and a wash period of 2 min between applications. Only one agonist was tested on each cell. When this protocol was repeated in low divalent solution, it was noted that repeated applications of ATP or Bz-ATP resulted in successively larger inward currents (see Results section). To minimize this effect, application times for agonists were reduced to 0.5 s. For both agonists, the effects of the P2 receptor antagonists, suramin (100 μM), and pyridoxal-phosphate-6-azophenyl-2′, 4′-disulphonic acid (PPADS; 30 μM), were investigated by continuous perfusion of antagonist for 10 min before and during determination of a second agonist concentration-effect curve.

In order to investigate the augmentation in inward currents caused by successive applications of ATP in low divalent solution, ATP (1 mM) was repeatedly applied for 1 s to each naïve cell. This was repeated up to 20 times, with a 30 s wash period between successive applications. This protocol was used to investigate the ability of suramin (100 μM), PPADS (30 μM), or 5-(N,N-hexamethylene)- amiloride (HMA; 100 μM) to slow or accelerate current augmentation. In each case a test application of 1 mM ATP alone was followed by repeated application of ATP in the continued presence of the agent under investigation. A pre-incubation period of at least 10 min was employed for the study of the effects of suramin or PPADS, but not for HMA. A new coverslip was used for each experiment.

A similar protocol was used to determined whether current augmentation occurred in normal divalent cation containing solution at elevated temperatures. By use of a heated water-jacket, repeated applications of 1 mM ATP were performed at bath temperatures of 23, 27 and 32°C.

In low divalent solution, following a 30 s application of 1 mM ATP, during which maximal current augmentation was observed, concentration-effect curves were constructed for ATP, Bz-ATP, 2MeS-ATP, or α,β-methylene adenosine 5′-triphosphate ($\alpha\beta$meATP), by application of these agonists for 2 s, with a 2 min wash period between successive applications. The effects of suramin (100 μM), PPADS (30 μM) and HMA (100 μM) were investigated as described above, with a 10 min pre-incubation period between determination of first and second concentration-effect curves. In a separate set of experiments, the action of the ATP derivative, oxidized ATP (ox-ATP), was investigated by pre-incubation of coverslips in normal divalent solution containing 300 μM ox-ATP for 2 h at 37°C before the recording.

The actions of the P2 receptor antagonists, reactive blue-2, coomassie blue-R and coomassie blue-G, were investigated on cells which had been pre-exposed to 1 mM ATP for 30 s in low divalent solution. ATP (1 mM) was then applied to cells for 2 s, followed by continuous perfusion of the antagonist under investigation for 5 min. A second application of ATP was performed in the presence of antagonist, followed by a 5 and 10 min wash period, at which times further test applications of ATP were performed.

In some cases, 5 mV hyperpolarizing voltage steps were applied for 20 ms, every 100 ms during each acquisition episode to determine membrane conductance. Current-voltage relationships for ATP-induced currents were also determined in some cells by performing voltage ramps from $-$90 to $+$60 mV in a 400 ms sweep, both in the absence and presence of 1 or 3 mM ATP.

Data are expressed as mean$\pm$s.e.mean absolute current evoked by nucleotides and analogues, mean percentage of the current evoked by 1 mM ATP, or mean percentage of the maximal inward current observed in a particular experimental paradigm. Where appropriate, concentration-effect curves were fitted with a four parameter logistic equation (GraphPad Prism, San Diego, CA, U.S.A.). EC_{50} values are expressed as geometric means with 95% confidence intervals. Differences in mean values were tested by use of Student's paired or unpaired t test, as specified in the text.

Ethidium bromide uptake

The ability of ATP to cause permeabilization of microglial cells, with subsequent uptake of ethidium bromide was tested by incubating coverslips in low divalent cation buffer con-

taining 20 μg ml^{-1} ethidium bromide, in the absence or presence of 1 mM ATP. Following a 30 s contact time, coverslips were washed twice with the low divalent buffer, and fluorescent cells were visualized by a Optiphot (Nikon) microscope with an epiflourescence attachment. The same experiments were also performed in normal divalent solution with an incubation temperature of 32°C.

Materials

Dulbecco's modified Eagle medium (DMEM), foetal calf serum, N-2 supplement and trypsin-EDTA solution were all obtained from GibcoBRL (Paisley, Scotland). Adenosine 5′-triphosphate (ATP), 2′- and 3′-O-(4-benzoylbenzoyl)-ATP, α,β-methylene ATP ($\alpha\beta$meATP), 5-(N-N-hexamethylene)-amiloride, basic fibroblast growth factor (bFGF), oxidized ATP (ox-ATP), amiloride and hexamethyleneimine were all obtained from Sigma (Poole, U.K.). 2-Methylthio-ATP was obtained from RBI (Herts, U.K.). Pyridoxal-phosphate-6-azophenyl-2′, 4′-disulphonic acid was obtained from Cookson (Southampton, U.K.). Ethidium bromide was obtained from Appligene (Co. Durham, U.K.). Suramin was a kind gift from Bayer. All other chemicals were purchased from Sigma or BDH Laboratory Supplies (Leicester, U.K.).

Results

Electrophysiological characteristics

Recordings were made from 288 NTW8 cells. The mean resting membrane potential was -51.2 ± 2.1 mV, with a mean cell capacitance of 29.6 ± 2.0 pF ($n=41$). The mean series resistance was 8.6 ± 0.4 MΩ, which was compensated by at least 80%.

Effects of agonists

At room temperature (23°C), in normal divalent cation containing solution, Bz-ATP and ATP evoked whole-cell inward currents at a holding potential of -90 mV in all NTW8 cells tested, with Bz-ATP being more potent than ATP. At the highest concentrations of these agonists tested (300 μM for Bz-ATP and 3 mM for ATP), inward currents were 549 ± 191 and 644 ± 198 pA, respectively ($n=9$ and 14). Concentration-effect curves to these agonists did not reach maxima, and thus EC_{50} values could not be determined (Figure 1). No significant tachyphylaxis or current augmentation was observed for either agonist with up to 5 applications at the highest concentrations (e.g. inward current elicited by fifth application of 1 mM ATP; 103.2 ± 6.2% of that elicited by the first application). Current-voltage relationships generated with 3 mM ATP were approximately linear between -60 and $+50$ mV, and reversed at 4.6 ± 3.0 mV ($n=4$; Figure 1b). At the highest concentration of 2MeS-ATP tested (300 μM), which was also the threshold concentration for observable responses with this agonist, evoked inward currents were no greater than 60 pA in any cell tested.

In low divalent solution, application of 1 mM ATP for 2 s produced inward currents which did not reach a maximum, but continued to increase in amplitude until the agonist was removed. Subsequent application of this ATP concentration produced successively larger currents. Shorter agonist application times minimized this effect and concentration-effect curves to Bz-ATP and ATP were determined with 0.5 s agonist applications. These currents were associated with an increase in membrane conductance (increasing from a resting conductance of 6.6 ± 2.0 to 65.2 ± 9.6 nS in 3 mM ATP). Inward currents recorded for second concentration-effect curves in the same cells were significantly larger than those observed for first curves for both agonists (Figure 2). Maximal currents obtained from the second concentration-effect curves to Bz-ATP and ATP were 1304 ± 378 and 2347 ± 310 pA, respectively (increase to 157.1 ± 30.0 and 128.2 ± 8.0%, $P<0.05$ for both agonists, Student's paired t test; Figure 2).

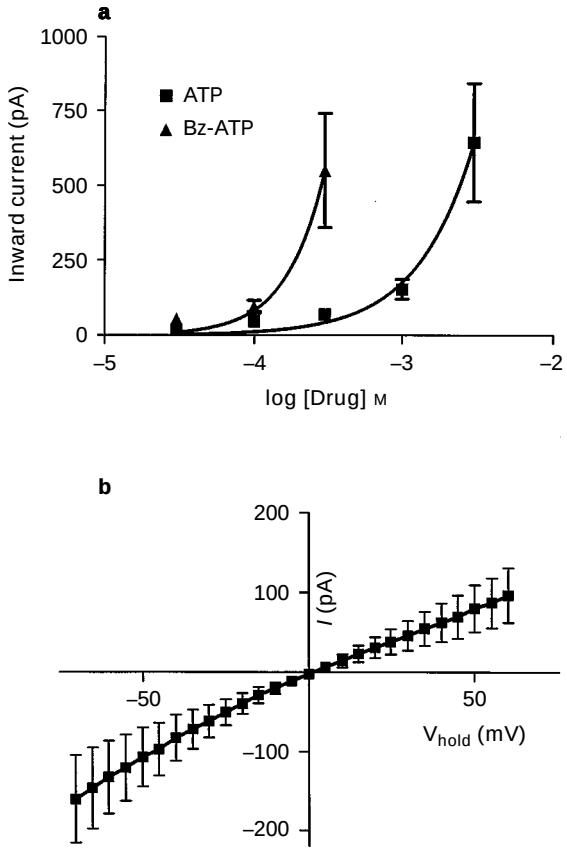

Figure 1 Characteristics of nucleotide-evoked responses in normal divalent cation containing solution. (a) Concentration-effect curves for Bz-ATP ($n=9$) and ATP ($n=14$). Agonists were applied for 2 s, with a wash period of 2 min between applications. (b) Current-voltage relationships for responses to 3 mM ATP, generated by a voltage ramp over a 400 ms period. For each cell, the mean of two control ramps was subtracted from the mean of two ramps generated in the presence of agonist ($n=4$). Data points are the means of n determinations; vertical lines show s.e.mean.

In a separate series of experiments, concentration-effect curves were determined following a 30 s appliction of 1 mM ATP, during which maximal steady-state currents were observed. Subsequent application of Bz-ATP or ATP produced large concentration-dependent steady-state currents (Figure 2). Calculated EC_{50} values for Bz-ATP, ATP and 2MeS-ATP were (95% confidence intervals in parentheses): 58.3 (46.1–73.9) μM, $n=11$; 298 (255–347) μM, $n=26$ and 505 (460–554) μM, $n=5$, respectively (Figure 3). The agonist $\alpha\beta$meATP produced only small inward currents even at the highest concentration tested (1 mM). As observed in normal divalent solution, current-voltage relationships for 1 mM ATP did not display strong rectification and reversed at 4.9 ± 0.7 mV (Figure 2).

Effects of antagonists

In low divalent solution, with brief (0.5 s) applications of ATP, suramin (100 μM), continuously perfused for 10 min before and during determination of a second concentration-effect curve, did not affect the increase in current recorded between curves (second curve maximum 152.3 ± 15.0% of first curve maximum at 3 mM ATP; Figure 4a). Similarly, suramin had no effect when applied between successive concentration-effect curves determined in cells which had been pre-exposed to 1 mM ATP for 30 s (Figure 4).

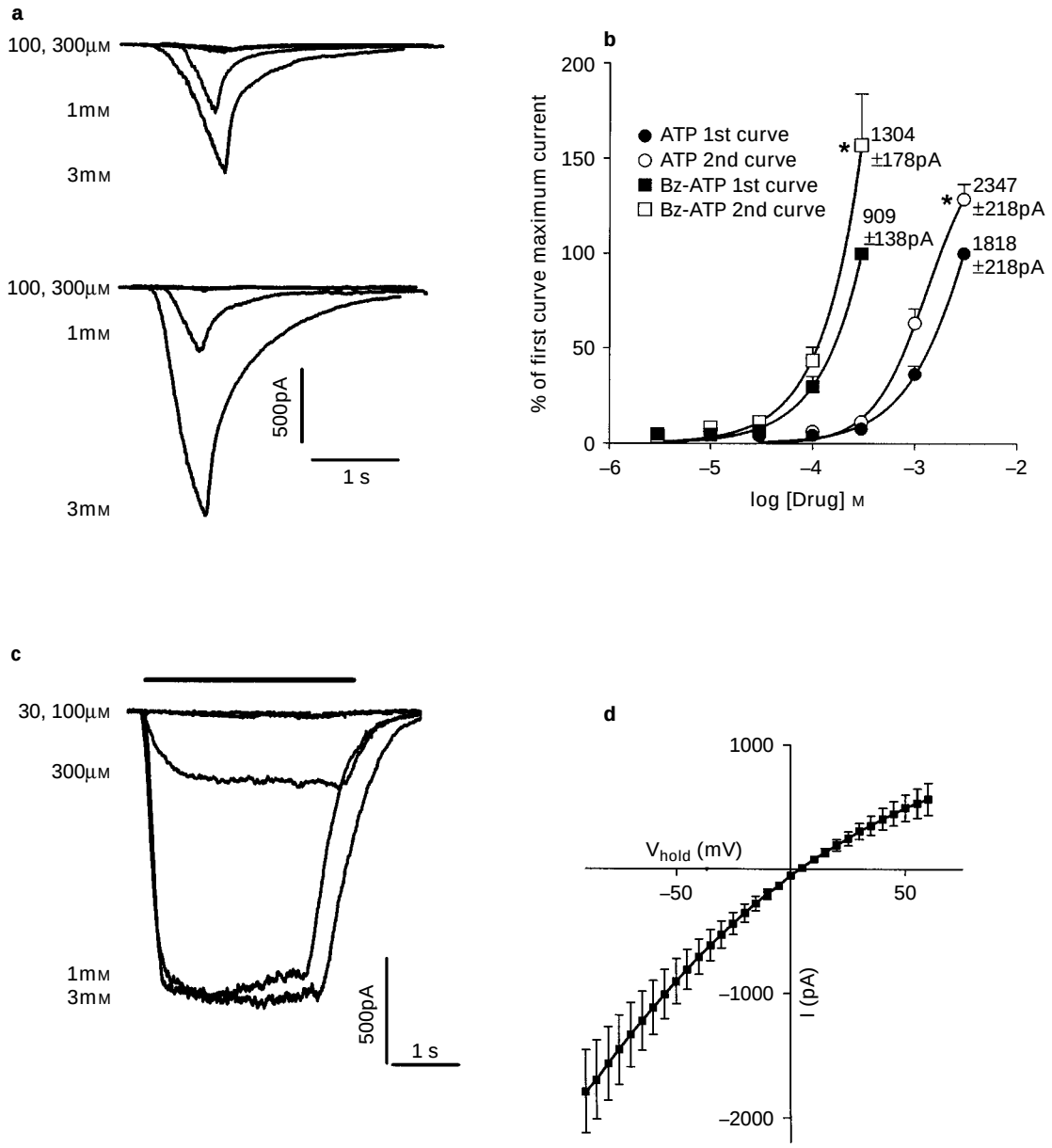

Figure 2 Characteristics of nucleotide-evoked responses in low divalent solution. (a) Brief application of ATP (0.5 s; concentrations 100 and 300 μM, 1 and 3 mM in both traces) - evoked inward currents (upper trace) which were larger in magnitude upon application of these concentrations a second time (lower trace). (b) First (solid symbols) and second (open symbols) concentration-effect curves for Bz-ATP ($n=9$) and ATP ($n=10$) with brief agonist applications, with 2 min between applications and 5 min between curves. Figures by 3 mM data points show mean maximum inward currents (pA). (c) Following application of ATP (1 mM) for 30 s, during which time maximal steady-state currents were observed, subsequent ATP applications for 2 s then produced large, plateauing inward currents. Concentrations of ATP are shown adjacent to traces. (d) Current-voltage relationships for responses to 1 mM ATP, generated by a voltage ramp over a 400 ms period. For each cell, the mean of two control ramps was subtracted from the mean of two ramps generated in the presence of agonist ($n=5$). Data points in (b) and (d) are the means of n determinations; vertical lines show s.e.mean. *$P<0.05$, significantly different from first curve maximum (Student's paired t test).

5-(N,N-hexamethylene)- amiroride (100 μM), which has been shown to block pore formation at some P2Z purinoceptors (Nuttle & Dubyak, 1994) was also ineffective at blocking inward currents when these protocols were used. However, with brief ATP applications (0.5 s), the augmentation of currents observed between successive concentration-effect curves to ATP was significantly enhanced in the presence of HMA (Figure 4c). The difference in maxima between curves in the presence of HMA was 198.8±17.5% at 3 mM ATP ($n=6$), compared with 128.2±8.0 in the absence of HMA ($n=7$; $P<0.05$, Student's unpaired t test). HMA had no effect on concentration-effect curves determined from cells which had been pre-exposed to 1 mM ATP for 30 s (EC_{50} values 336.8 (236.1–480.3) and 224.7 (156.1–323.5) μM, absence and presence of HMA, respectively; second curve maximum 102.1±26.0% of first curve maximum, $n=7$; Figure 4).

In contrast, PPADS (30 μM) prevented the augmentation of inward current observed between successive concentration effect curves such that the maxima obtained for second concentration-effect curves were significantly smaller than those observed for the first curve (second curve maximum 47.3±11.1% of the first at 3 mM, $P<0.05$, $n=6$; Figure 4). In addition, when this antagonist was tested on cells which had been pre-exposed to 1 mM ATP for 30 s, PPADS also significantly reduced the maximum response obtained with 3 mM ATP (second curve maximum 67.8±2.8% of that of the first,

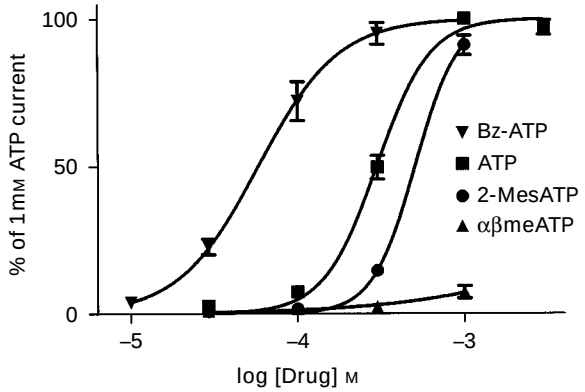

Figure 3 Concentration-effect curves in low divalent solution for Bz-ATP ($n=11$), ATP ($n=26$), 2-MesATP ($n=5$) and $\alpha\beta$meATP ($n=6$) following pre-exposure of cells to 1 mM ATP for 30 s. Data points are expressed as the mean percentage of inward currents obtained from two test applications of 1 mM ATP; vertical lines show s.e.mean. These mean current values for each curve were: -2616 ± 344, -3086 ± 399, -2990 ± 257 and -3146 ± 401 pA for Bz-ATP, ATP, 2-MesATP and $\alpha\beta$meATP, respectively.

$P<0.05$, $n=6$; Figure 4), but did not significantly alter the agonist EC_{50} value (419.7 (266.2–661.6) and 813.5 (253.1–2615.0) μM, absence and presence of PPADS, respectively; Figure 4).

Incubation of coverslips with 300 μM ox-ATP for 2 h at 37°C abolished ATP-evoked inward currents in all cells tested, both in normal and low divalent solution ($n=6$ for both conditions), such that no discernible currents were observed at any concentration of ATP tested.

The P2 receptor antagonists, coomassie brilliant-blue-R (CBB-R; 30 μM), coomassie brilliant-blue-G (CBB-G; 10 μM), and reactive blue-2 (RB-2; 30 μM), all caused inhibition of ATP (1 mM) -evoked currents when tested on cells which had been pre-exposed to 1 mM ATP for 30 s (Table 1). Of these three antagonists, only the effects of reactive blue-2 were reversible.

Current augmentation

In low divalent solution at room temperature, repeated applications of ATP (1 mM) for 1 s produced successively larger inward currents (Figure 5), which reached a plateau after 8 applications of $466\pm52\%$ of the first application current ($n=26$; Figure 5). When PPADS (30 μM) was continuously perfused for 10 min after the first application, augmentation was blocked (Figure 5), with no significant difference in the magnitude of inward current between the first and the twentieth application in the presence of PPADS ($n=7$). This was associated with a significant reduction in inward current between applications of ATP in the absence and presence of PPADS (reduction to $61.3\pm8.0\%$ of the first application current in the absence of PPADS, and the second application in the presence of PPADS). Suramin (100 μM), when applied in the same way, had no inhibitory effect on current magnitude, or the number of applications required to reach a plateau ($584\pm127\%$ of first current after 8 applications; $n=6$).

HMA (100 μM) significantly accelerated current augmentation; a maximal current plateau was reached after only one application of ATP in the presence of HMA (increase to $439\pm34\%$ of the first ATP current in the absence of HMA; Figure 5b and 5c). This effect was noted whether HMA was continuously perfused before successive ATP applications, or co-applied with ATP from the U-tube system with no pre-incubation. HMA had no effect when applied alone and acceleration of augmentation was not observed when ATP was applied in the presence of vehicle. When a control application of ATP was followed by one application of ATP with HMA, and then ATP alone, no further augmentation was observed (data not shown). Current augmentation in the presence of amiloride (100 μM) or hexamethyleneimine (100 μM) was not significantly different from that observed in the absence of these agents (data not shown).

In normal divalent solution at room temperature, successive application of ATP (1 mM) produced similar, small inward currents (Figure 6). However, elevation of the bath temperature to 27 and 32°C revealed the augmentation phenomena seen in the absence of divalent cations (Figure 6). At room temperature in normal divalent solution, HMA did not cause immediate and maximal augmentation, but potentiated ATP-evoked currents to a maximum of $214.6\pm29.5\%$ of the current obtained with ATP in the absence of HMA.

Ethidium bromide uptake

In the same low divalent cation containing buffer used in the electrophysiological experiments, application of 1 mM ATP for 30 s caused marked cellular uptake of ethidium bromide, such that approximately 95% of all cells displayed a strong fluorescent (Figure 7), while less than 5% of cells displayed strong fluorescence when incubations were performed in ethidium bromide in the absence of ATP. In normal divalent solution when incubations were performed at 32°C, ATP (1 mM) also caused marked uptake of ethidium bromide (Figure 7).

Discussion

In this study, we have used whole-cell patch-clamping methods to characterize the properties of an endogenous purinoceptor subtype, the pharmacology of which resembles the recently cloned P2X$_7$ (previously termed P2Z) receptor (Surprenant *et al*., 1996). We have investigated these pharmacological properties with a variety of nucleotide analogues and studied the electrophysiological characteristics of ATP-induced current augmentation.

In extracellular solution containing 2 mM Ca^{2+} and 1 mM Mg^{2+}, the rank order of agonist potency was Bz-ATP > ATP > 2MeS-ATP. In low divalent solution, containing 0.5 mM Ca^{2+} and zero Mg^{2+}, the inward current evoked by ATP was larger and the relative agonist potencies were not significantly altered. The P2X receptor agonist, $\alpha\beta$meATP, was almost ineffective. ATP-evoked currents were insensitive to the P2 receptor antagonist, suramin, but were significantly antagonized by PPADS. Oxidized ATP irreversibly blocked inward current, provided cells were pre-incubated for 2 h or more. This pharmacological profile is typical of the previously described P2Z purinoceptor (Murgia *et al*., 1993; Nuttle & Dubyak, 1994; Ferrari *et al*., 1996), and the recently described recombinant P2X$_7$ receptor (Surprenant *et al*., 1996). The presence of this receptor type in primary microglial cells has been previously described (Haas *et al*., 1996; Ferrari *et al*., 1996) and P2X receptors other than P2X$_7$ have also been noted (Walz *et al*., 1993; Nörenberg *et al*., 1994). In the present study, we found no evidence for any P2X receptor, other than P2X$_7$ in the NTW8 cell line. Although P2Y receptors have also been found in primary microglial cells (Nörenberg *et al*., 1994), their possible electrophysiological effects were excluded in the present study by the inclusion of caesium in all intracellular solutions.

It has been suggested that ATP^{4-} is the active species at the P2Z receptor, as ATP responses are inhibited in the presence of Mg^{2+} (Nuttle & Dubyak, 1994). This was also noted in the present study, where responses recorded in extracellular solutions with lowered concentrations of divalent cations were of greater amplitude than those recorded in normal extracellular solution. More significantly, the phenomenon of current augmentation was not noted in normal extracellular solution at room temperature, but in low divalent solution, continued application of high concentrations of ATP gave rise to a steadily increasing inward current, reaching a plateau after 15–20 s application of ATP (1 mM), which deactivated when

ATP was removed. In separate experiments, 1 s pulses of ATP gave rise to successively larger ligand-gated inward currents which reached a plateau after approximately eight such applications. This effect did not reverse during the course of each experiment; once a maximum current had been noted, approximately equal ligand-gated currents were achieved after up to 40 min of washing (unpublished observations). We propose that these large currents reflect formation and gating of the large membrane pores, characteristic of P2Z receptors, which are formed and activated by high concentrations of ATP (see Introduction). It is known that various cell types, including microglial cells, can be permeabilized by use of ATP (Heppel *et al*., 1985; Steinberg *et al*., 1987; Ferrari *et al*., 1996), resulting in uptake or release of large molecules such as ethidium bromide, which has a molecular weight of 394 Da (Tatham & Lindau, 1990; Ferrari *et al*., 1996). Indeed in our studies, a 30 s application of ATP in low divalent solution caused uptake of ethidium bromide in approximately 95% of cells, while very

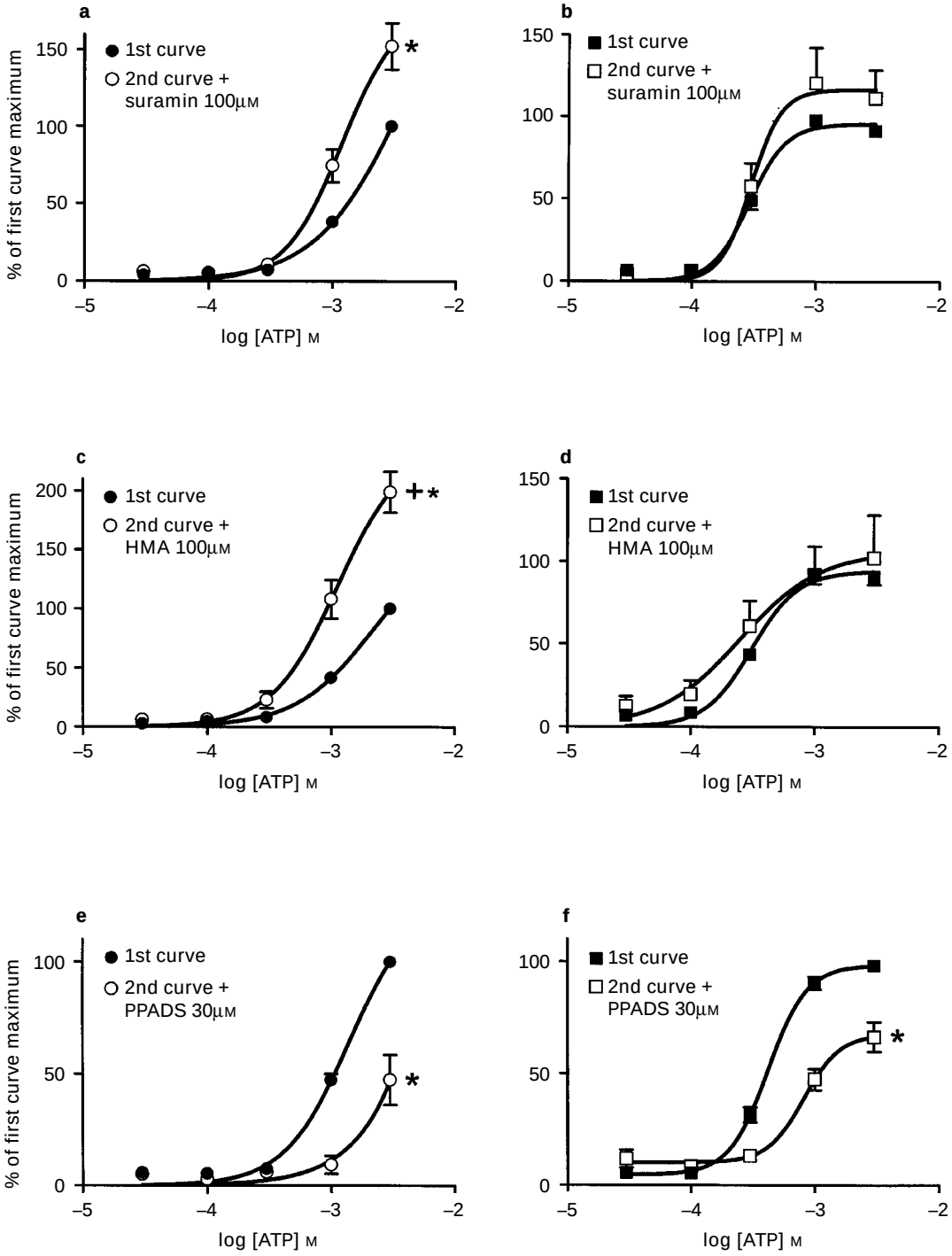

Figure 4 Effects of antagonists on ATP-evoked responses. In all cases, first concentration-effect curves (solid symbols) were followed by a determination of a second concentration-effect curve (open symbols) in the continued presence of suramin 100 μM (a and b), HMA 100 μM (c and d) or PPADS 30 μM (e and f). Incubation times with antagonists between curves were 10 min. The left column (a, c and e) shows effects of antagonists on curves generated by brief (0.5 s) ATP application. The right column (b, d and f) shows effects of antagonists on concentration-effect curves from cells which had been pre-exposed to ATP (1 mM) for 30 s. Agonist application times were 2 s. Each data point represents determinations from at least 6 cells; vertical lines show s.e.mean. For all figures, 100% values relate to inward currents of: 1234$\pm$325, 1533$\pm$262, 872$\pm$147, 2126$\pm$537, 886$\pm$138 and 1673$\pm$422 pA (a to f, respectively). *$P<0.05$, significantly different from corresponding first curve maximum (Student's paired t test). $^{+}P<0.05$, significantly different from the difference observed between first and second curve maxima in control experiments (Student's unpaired t test).

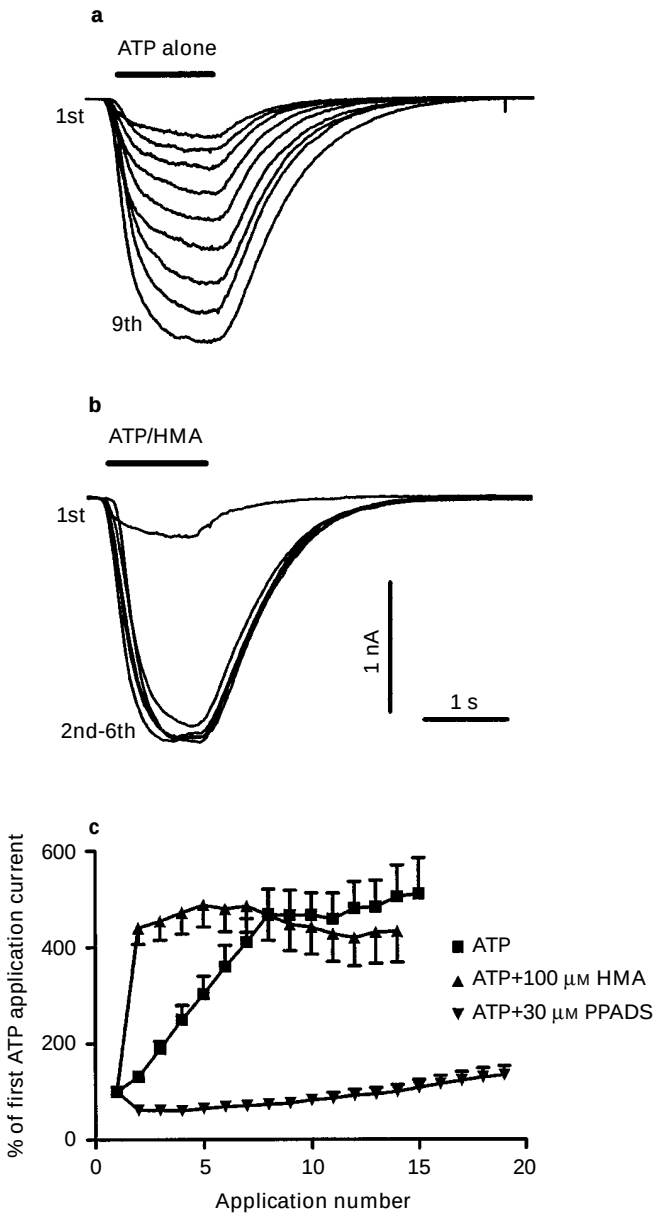

Figure 5 Characteristics of current augmentation in low divalent solution. (a) Inward currents evoked by 9 successive applications of 1 mM ATP at room temperature. (b) Inward currents evoked by ATP alone (first application) followed by ATP in the presence of 100 μM HMA. (c) Current augmentation caused by repeated applications of 1 mM ATP alone ($n=26$), ATP in the presence of HMA ($n=17$) and ATP in the presence of PPADS ($n=7$). In all cases, data are expressed as the mean percentage of the response to the first application of ATP, which was always made in the absence of any other agents: vertical lines show s.e.mean. Initial currents for each curve were (100% values): -429 ± 46, -419 ± 48 and -382 ± 23 pA for ATP alone, ATP followed by HMA and ATP followed by PPADS, respectively.

few fluorescent cells were observed in the absence of ATP. In keeping with previous findings, our electrophysiological data also indicated induction of 'pore formation' in normal divalent solution at increased temperature (Nuttle & Dubyak, 1994), suggesting that *in vivo*, this phenomenon may have physiological significance. Thus, the findings in our study would seem to indicate that ATP-induced permeabilization, mediated via P2X$_7$ receptors, can be directly observed by voltage-clamp measurements in mouse microglial cells.

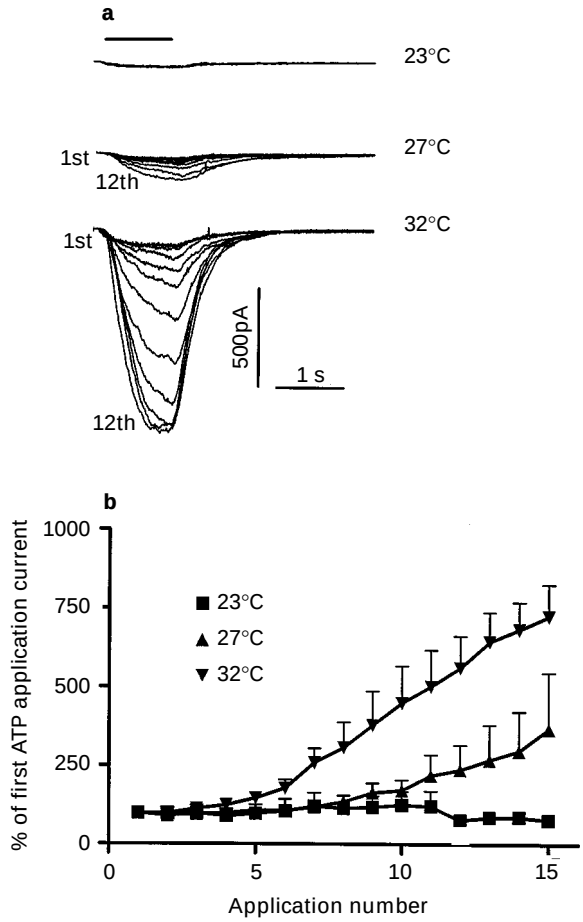

Figure 6 Characteristics of current augmentation in normal divalent solution. (a) Repeated applications of 1 mM ATP at various bath temperatures. The upper trace shows responses to application numbers, 1, 4, 6, 8, 10 and 12 at 23°C. The middle and lower traces show responses to 12 consecutive applications at 27 and 32°C. (b) Current augmentation caused by repeated applications of 1 mM ATP alone at 23°C ($n=8$), 27°C ($n=5$) and 32°C ($n=6$). In each case, data are expressed as the mean percentage of the response evoked by a first application of ATP alone; vertical lines show s.e.mean. Initial currents to 1 mM ATP were (100% values): 39.3 ± 5.3, 51.8 ± 13.0 and 79.0 ± 14.0 pA for currents obtained at 23, 27 and 32°C, respectively.

Table 1 Effects of the P2 antagonists, Coomassie brilliant blue -R and -G (CBB-R and CBB-G) and reactive blue-2 (RB-2), on ATP-evoked current in NTW8 cells pre-exposed to 1 mM ATP for 30 s

	Control	*CBB-R* 30 μM	*CBB-G* 10 μM	*RB-2* 30 μM
First Current (pA)	1382 ± 221	1866 ± 547	1390 ± 290	2042 ± 371
+Antagonist (% of 1st current)	101.2 ± 4.7	53.0 ± 10.0*	25.0 ± 3.2*	32.6 ± 6.4*
5 min wash (% of 1st current)	95.8 ± 5.2	59.8 ± 1.4*	39.7 ± 4.7*	93.1 ± 23.6
15 min wash (% of 1st current)	96.1 ± 5.3	50.9 ± 5.1*	49.4 ± 4.6*	
n	9	4	5	5

All antagonists were continuously perfused for 5 min and co-applied with ATP (1 mM) following the first application of ATP. Two further agonist applications were made following a 5 and 15 min wash. Control data were generated by use of the same protocol without antagonist additions. *$P<0.05$, significantly different from first application current, Student's paired *t* test.

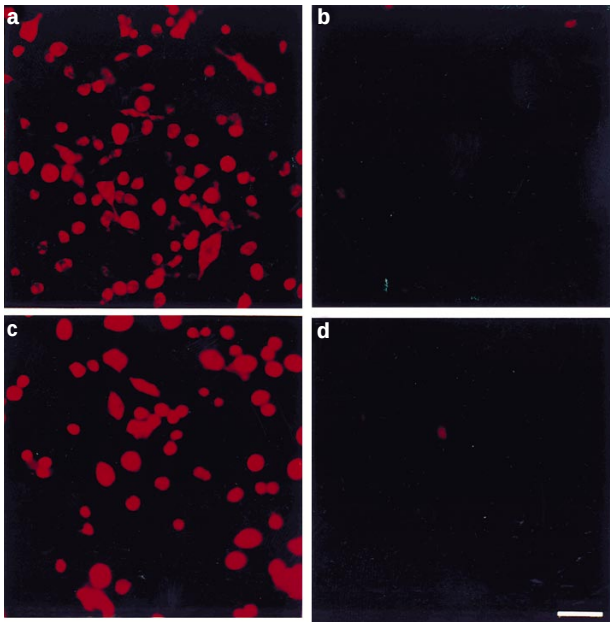

Figure 7 Photomicrograph of fluorescent images of NTW8 cells. (a) Cells incubated for 30 s in low divalent solution containing 20 μg ml^{-1} ethidium bromide in the presence or absence (b) of 1 mM ATP, at room temperature. (c) Cells incubated as above in normal divalent solution at 32°C in the presence or absence (d) of 1 mM ATP. Scale bar in (d) 400 μm.

The P2 receptor antagonist, PPADS, inhibited currents evoked by brief ATP applications, as well as inward currents in cells which had been pre-exposed to 1 mM ATP for 30 s, which as discussed above, was sufficient to cause pore formation in these cells. PPADS also inhibited initiation of pore formation when applied after the first application of 1 mM ATP. This suggested that pore formation might be dependent upon channel ion-flux. However in other experiments when ATP was applied while cells were voltage clamped at the channel reversal potential, a second application of ATP at a holding potential of −90 mV evoked a large non-potentiating steady-state current, suggesting that net ion flux *per se* is not responsible for pore formation (unpublished observations).

HMA appeared to cause rapid induction of pore formation in the presence of ATP; HMA had no effect when applied alone, but when applied with ATP, it caused immediate and maximal augmentation of inward currents. This action of HMA appeared to be rapid, as no differences in its effects were observed whether cells were pre-incubated with HMA for 10 min, or if HMA and ATP were co-applied with no pre-exposure. In contrast, in normal divalent cation containing solution at room temperature, HMA cuased only moderate potentiation of ATP-mediated responses. The action of HMA in low divalent solution was unexpected, as several other studies have shown that this compound blocks ATP-mediated ion flux, ATP-mediated inward currents and fluorescent dye uptake (Wiley *et al*., 1990, 1992; Nuttle & Dubyak, 1994). The reasons for this descrepancy are not clear, although there are a number of possibilities. First, HMA is known to quench fluorescent signals strongly from certain dyes (Nuttle & Dubyak, 1994) and, as such, may mask fluorescent indices of pore formation. Second, previous studies on the effects of HMA were carried out in different species and it is known that the characteristics of the P2X$_7$ receptor differ between species. For example, in murine macrophages, Bz-ATP is the most potent agonist at this receptor, whilst in human macrophages, Bz-ATP is of equal or lesser potency than ATP itself (Hickman *et al*., 1994; Surprenant *et al*., 1996). Third, it is possible that these ATP receptors are composed of different heteropolymeric combinations which vary between cell types, conferring different pharmacological profiles. To our knowledge, this is the first time that the actions of HMA on pore formation have been studied in mouse microglial cells and additional study and comparison of effects between cell types is required to explore its effects further.

In common with RB-2 (cibacron blue 3GA), the aromatic sulphonic acids, CBB-G and CBB-R, both caused inhibition of currents recorded from cells in which pore formation had been induced. CBB-G was more effective than CBB-R, reducing inward currents by approximately 75% at a concentration of 10 μM, compared with 47% for CBB-R at a concentration of 30 μM. Both antagonists were only partially reversible after 15 min of washing. By contrast, inhibitory effects caused by the non-selective P2 receptor antagonist, RB-2, were rapidly reversible after only 5 min of washing.

Microglia are thought to be involved in the pathogenesis of several neurodegenerative diseases (see Introduction). As well as their benign action of phagocytosing debris and dead cells, microglia are capable of mediating cytotoxic actions by a variety of means. When activated, microglia can release TNF-α and NO as well as several reactive oxygen species. All of these agents have been shown to kill neurones in certain circumstances (see Chao *et al*., 1996a). In addition, interleukin-1β (IL-1β), produced by activated microglia, is also able to cause neuronal death (Chao *et al*., 1996b), but IL-1β is not released in a biologically active form from microglia and macrophages unless stimulated by ATP (Perregaux & Gabel, 1994). Although any role which ATP might play in mediating microglial associated toxicity is far from clear, it is possible that the ATP receptor described in the present study plays a part in controlling microglial responses and proliferation.

In summary, we have demonstrated that mouse NTW8 microglial cells possess a purinoceptor with pharmacological characteristics resembling the P2X$_7$ receptor. Using electrophysiological techniques, we have provided evidence that it is possible to monitor formation of the cytolytic pore, characteristic of this receptor and that pore formation can be modulated by use of pharmacological manipulations. Furthermore, we have shown that in more physiologically relevant conditions (divalent cation containing solutions and elevated temperature), pore formation can occur. Further study is required to determine the role (if any) that this and other purinoceptors may play in microglia activation in physiological and/or pathological events.

We gratefully acknowledge Dr H.T.R. Rupniak for supply of the NTW8 cell line and Dr I.K. Anderson for helpful discussion.

References

ANDERSON, I.K., CHOUDRY, S., WASLIDGE, N. & RUPNIAK, H.T.R. (1997). Immunohistochemical and functional characterisation of NTW8 microglial cells. *Br. J. Pharmacol.*, **120,** 272P.

CHAO, C.C., HU, S. & PETERSON, P.K. (1996a) Glia: the not so innocent bystanders. *J. Neurovirol.*, **2,** 234–239.

CHAO, C.C., HU, S., SHENG, W.S., BU, D., BUKRINSKY, M.I. & PETERSON, P.K. (1996b). Cytokine-stimulated astrocytes damage human neurones via a nitric oxide mechanism. *Glia*, **16,** 276–284.

CHESSELL, I.P., ANDERSON, I.K., RUPNIAK, H.T.R. & HUMPHREY, P.P.A. (1997). Pharmacological properties of microglial P2X$_7$ purinoceptors. *Br. J. Pharmacol.*, **120,** 127P.

CHIOZZI, P., MURGIA, M., FALZONI, S., FERRARI, D. & DI VIRGILIO, F. (1996). Role of the P2Z receptor in spontaneous cell death in J774 macrophage cultures. *Biochem. Biophys. Res. Commun.*, **218,** 176–181.

COCKROFT, S. & GOMPERTS, B.D. (1979). ATP induces nucleotide permeability in rat mast cells. *Nature*, **279,** 541 – 542.

EDWARDS, F.A., GIBB, A.J. & COLQUHOUN, D. (1992). ATP receptor-mediated synaptic currents in the central nervous system. *Nature*, **359,** 144 – 147.

FENWICK, E.M., MARTY, A. & NEHER, E. (1982). A patch-clamp study of bovine chromaffin cells and of their sensitivity to acetylcholine. *J. Physiol.*, **331,** 577 – 597.

FERRARI, D., VILLALBA, M., CHIOZZI, P., FALZONI, S., RICCIARDI-CASTAGNOLI, P. & DI VIRGILIO, F. (1996). Mouse microglial cells express a plasma membrane pore gated by extracellular ATP. *J. Immunol.*, **156,** 1531 – 1539.

FREDHOLM, B.B., ABBRACCHIO, M.P., BURNSTOCK, G., DALY, J.W., HARDEN, K., JACOBSON, K.A., LEFF, P. & WILLIAMS, M. (1994). VI. Nomenclature and classification of purinoceptors. *Pharmacol. Rev.* **46,** 143 – 156.

HAAS, S., BROCKHAUS, J., VERKHRATSKY, A. & KETTENMANN, H. (1996). ATP-induced membrane currents in ameboid microglia acutely isolated from mouse brain slices. *Neuroscience*, **75,** 257 – 261.

HAMILL, O.P., MARTY, A., NEHER, E., SAKMANN, B. & SIGWORTH, F.J. (1981). Improved patch-clamp techniques for high-resolution recording from cells and cell-free membranes. *Pflügers Arch.*, **391,** 85 – 100.

HEPPEL, L.A., WEISMAN, G.A. & FRIEDBERG, I. (1985). Permeabilization of transformed cells in culture by external ATP. *J. Membrane Biol.* **86,** 189 – 196.

HICKMAN, S.E., EL KHOURY, J., GREENBERG, S., SCHIEREN, I. & SILVERSTEIN, S.C. (1994). P2Z adenosine triphosphate receptor activity in cultured human monocyte-derived macrophages. *Blood*, **84,** 2452 – 5456.

HOFMAN, F.M., HINTON, D.R., JOHNSON, K. & MERRILL, J.E. (1989). Tumor necrosis factor identified in multiple sclerosis brain. *J. Exp. Med.*, **170,** 607 – 612.

KREUTZBERG, G.W. (1996). Microglia: a sensor for pathological events in the CNS. *Trends Neurosci.*, **19,** 312 – 318.

MCGEER, P.L., ITAGAKI, S., BOYES, B.E. & MCGEER, E.G. (1988). Reactive mictoglia are positive for HLA-DR in the substantia nigra of Parkinson's and Alzheimer's disease. *Neurology*, **38,** 1285 – 1291.

MCGEER, P.L. & MCGEER, E.G. (1995). The inflammatory response system of brain: implications for therapy of Alzheimer and other neurodegenerative diseases. *Brain Res. Rev.*, **21,** 195 – 218.

MURGIA, M., HANAU, S., PIZZO, P., RIPPA, M. & DI VIRGILIO, F. (1993). Oxidized ATP, an irreversible inhibitor of the macrophage purinergic P_{2Z} receptor. *J. Biol. Chem.*, **268,** 8199 – 8203.

NÖRENBERG, W., LANGOSCH, J.M., GEBICKE-HAERTER, P.J. & ILLES, P. (1994). Characterization and possible function of adenoxine 5′-triphosphate receptors in activated rat microglia. *Br. J. Pharmacol.*, **111,** 942 – 950.

NUTTLE, L.C. & DUBYAK, G.R. (1994). Differential activation of cation channels and non-selective pores by macrophage P_{2Z} purinergic receptors expressed in Xenopus oocytes. *J. Biol. Chem.*, **269,** 13988 – 13996.

PERREGAUX, D. & GABEL, C.A. (1994). Interleukin-1β maturation and release in response to ATP and nigericin. *J. Biol. Chem.*, **269,** 15195 – 15203.

PIZZO, P., MURGIA, M., ZAMBON, A., ZANOVELLO, P., BRONTE, V., PIETROBON, D. & DI VIRGILIO, F. (1992). Role of P_{2Z} purinergic receptors in ATP-mediated killing of tumor necrosis factor (TNF)-sensitive and TNF-resistant L929 fibroblasts. *J. Immunol.*, **149,** 3372 – 3378.

ROGERS, J., LUBER-NARDO, J., STYREN, S.D. & CIVIN, W.H. (1988). Expression of immune system-associated antigens by cells of the central nervous system: relationship to the pathology of Alzheimer's disease. *Neurobiol. Aging*, **9,** 339 – 349.

STEINBERG, T.H., NEWMAN, A.S., SWANSON, J.A. & SILVERSTEIN, S.C. (1987). ATP^{4-} permeabilizes the plasma membrane of mouse macrophages to fluorescent dyes. *J. Biol. Chem.*, **262,** 8884 – 8888.

SUPRENANT, A., RASSENDREN, F., KAWASHIMA, E., NORTH, R.A. & BUELL, G. (1996). The cytolytic P_{2Z} receptor for extracellular ATP identified as a P_{2X} receptor ($P2X_7$). *Science*, **272,** 735 – 738.

TATHAM, P.E.R., & LINDAU, M. (1990). ATP-induced pore formation in the plasma membrane of rat peritoneal mast cells. *J. Gen. Physiol.*, **95,** 459 – 476.

WALZ, W., ILSCHNER, S., OHLEMEYER, C., BANATI, R. & KETTENMANN, H. (1993). Extracellular ATP activates a cation conductance and a K^+ conductance in cultured microglial cells from mouse brain. *J. Neurosci.*, **13,** 4403 – 4411.

WIERASZKO, A., GOLDSMITH, G. & SEYFRIED, T.N. (1989). Stimulation-dependent release of adenosine triphosphate from hippocampal slices. *Brain Res.*, **485,** 244 – 250.

WILEY, J.S., JAMIESON, G.P., MAYGER, W., CRAGOE, E.J. & JOPSON, M. (1990). Extracellular ATP stimulates an amiloride-sensitive sodium influx in human lymphocytes. *Arch. Biochem. Biophys.*, **290,** 263 – 268.

WILEY, J.S., CHEN, R., WILEY, M.J. & JAMIESON, G.P. (1992). The ATP^{4-} receptor-operated ion channel of human lymphocytes: Inhibition of ion fluxes by amiloride analogues and by extracellular sodium ions. *Arch. Biochem. Biophys.*, **292,** 411 – 418.

(Received January 16, 1997
Revised April 21, 1997
Accepted April 24, 1997)